

4D Flow Imaging with UNFOLD in a Reduced Field-of-View

Clarissa Wink¹, Jean Pierre Bassenge^{1,2}, Giulio Ferrazzi¹, Tobias Schaeffter¹, Sebastian Schmitter¹

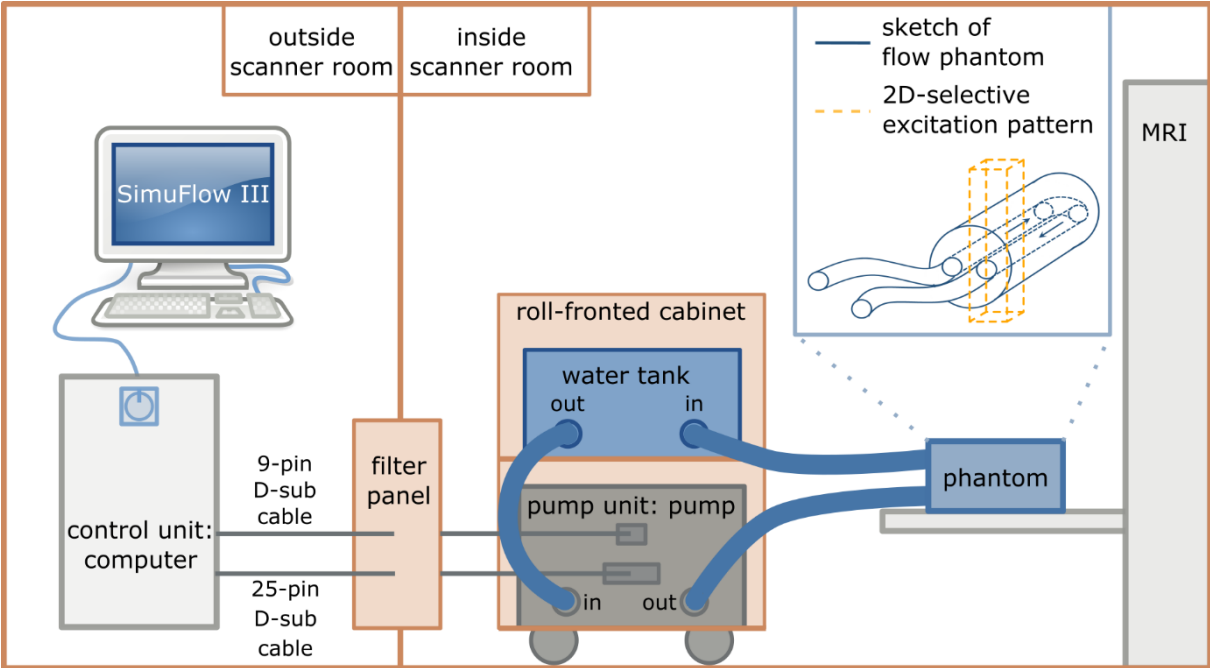
1. Physikalisch-Technische Bundesanstalt (PTB), Braunschweig and Berlin, Germany.
2. Working Group on Cardiovascular Magnetic Resonance, Experimental and Clinical Research Center, a joint cooperation between the Charité Medical Faculty and the Max-Delbrueck Center for Molecular Medicine.

Parts of this work have been presented at the 27th joint annual meeting ISMRM-ESMRMB (Abstract 3401).

Corresponding Author: Clarissa Wink
Department of Biomedical Magnetic Resonance
Physikalisch-Technische Bundesanstalt (PTB)
Abbestr. 2-12
10587 Berlin
Germany
Email: Clarissa.Wink@ptb.de

Supporting Information

Supporting Information Figure S1

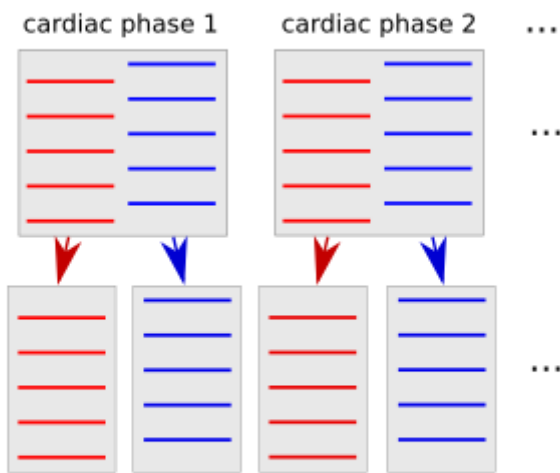


Supporting Information Figure S1: Illustration of the setup with flow phantom and the CardioFlow 5000 MR pulsatile flow pump (CardioFlow 5000 MR). The inlay shows a sketch of the flow phantom and the 2DRF pattern.

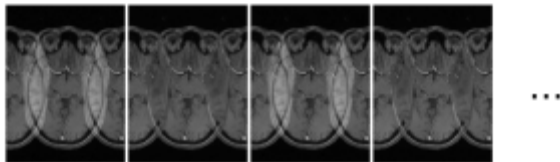
Supporting Information Figure S2

Illustration of UNFOLD data processing

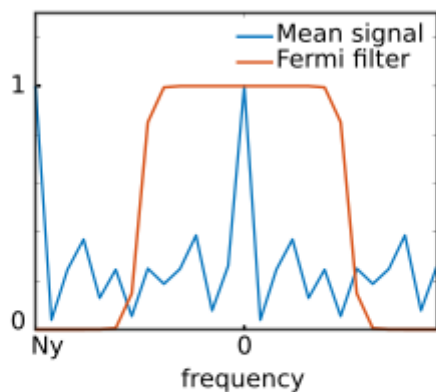
a split odd and even lines in separate phases



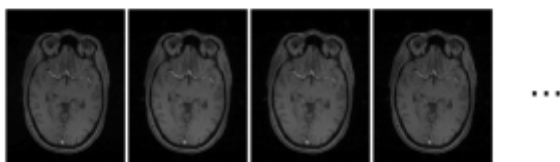
b Conventional reconstruction to image space



c FFT in time dimension & frequency filtering



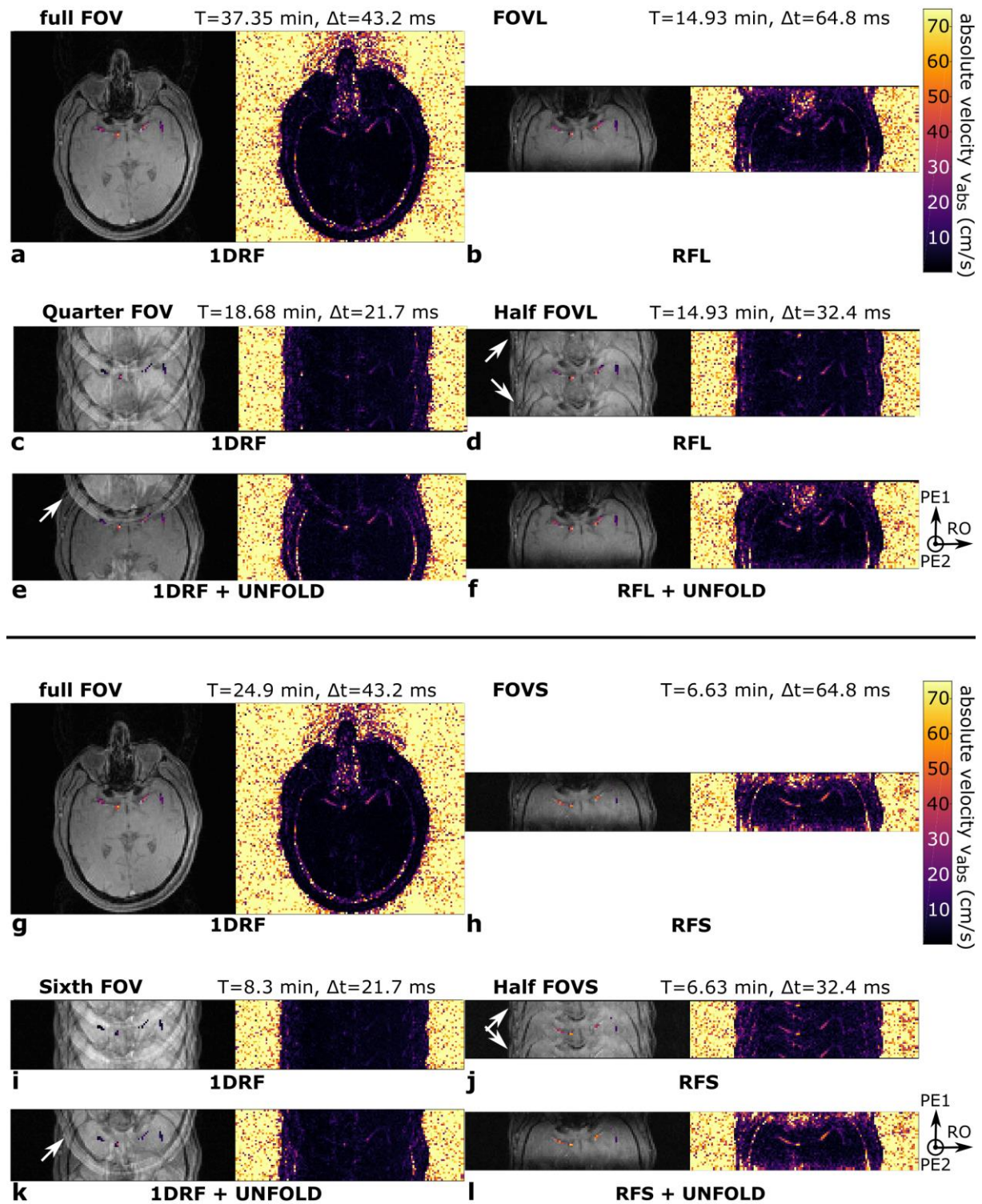
d IFFT in time dimension



Supporting Information Figure S2: Illustration of data processing with UNFOLD. **A**, The data of a sequence acquiring 2 k-space lines per cardiac phase were split into 2 separate phases. The set of k-space lines was then shifted by half a line from phase to phase. **B**, Every phase was Fourier-transformed to complex image space. The phase of the resulting complex aliasing

artifacts changes sign at the Nyquist frequency. **C**, A fast Fourier transform (FFT) was applied in the temporal dimension, and the resulting signal was filtered using a Fermi filter to remove the aliasing artefacts. **D**, The inverse FFT (iFFT) in the temporal dimension resulted in unaliased dynamic images that had nominally twice the temporal resolution.

Supporting Information Figure S3:

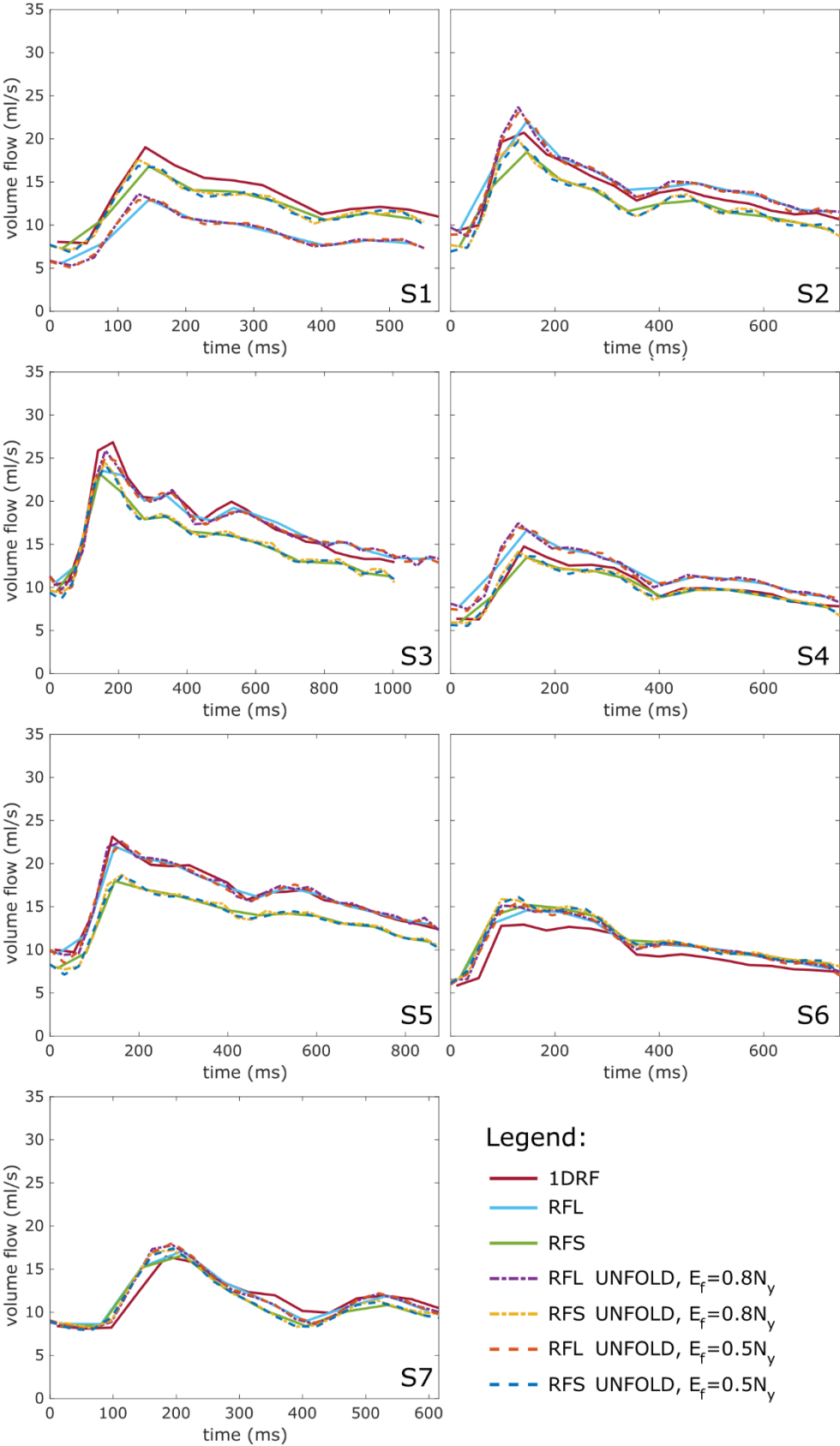


Supporting Information Figure S3: Systolic magnitude (gray) and absolute velocity 4D flow images (color) targeting the circle of Willis of subject S6 with different FOV sizes, 1DRF or 2DRF, and UNFOLD as indicated. The nominal acquisition time and nominal temporal resolution Δt are given in the headlines. **A**, Full FOV data (III) excited 1D selectively, and, **B**, full FOVL data (I) excited with RFL. **C**, **E**, Quarter FOV data (III^{4x}) and, **D**, **F**, half FOVL data (I^{2x}) reconstructed without (**C**, **D**) and with (**E**, **F**) UNFOLD. **G**, Full FOV data (III) excited 1D

selectively and, **H**, full FOVS data (II) excited with RFS. **I,K**, Sixth FOV data (III^{6x}) and, **J,L**, half FOVS data (II^{2x}) reconstructed without (**I,J**) and with (**K,L**) UNFOLD. The UNFOLD technique effectively removed the aliasing in data sets (I^{2x}) and (II^{2x}) near the edges of the reduced FOV (rFOV) (**D,J**, white arrows), resulting in image quality equivalent to conventionally reconstructed data sets (I) and (II) (**B,H**), but with doubled the nominal temporal resolution (**F,L**). Applying UNFOLD to data sets (III^{4x}) and (III^{6x}), however, removed only static first-order aliasing, whereas second-order aliasing remained visible (**E,K**, white arrow). Furthermore, the static aliasing in scans (I^{2x}) and (II^{2x}) near the edges of the rFOV (**D,J**, white arrows) indicates where dynamic aliasing may occur when the bandwidth of the data is larger than the UNFOLD Fermi filter. Abbreviations: FOVL= $256 \times 96 \times 96 \text{ mm}^3$, the rFOV adjusted to the FOX of RFL; FOVS = $256 \times 64 \times 64 \text{ mm}^3$, the rFOV adjusted to the FOX of RFS

Supporting Information Figure S4

**Time-resolved flow through internal carotid arteries,
with and without UNFOLD reconstruction**



Supporting Information Figure S4: Time-resolved flow curves through the internal carotid arteries of all subjects obtained with the 2DRF data sets (I and II) reconstructed without and with UNFOLD $E_f = 0.8 N_y$ and $E_f = 0.5 N_y$ and flow curves obtained with the 1DRF data set (III).

Supporting Information Table S1:

A Relative mean difference in peak flow between 1DRF excitation and 2DRF excitations RFL or RFS for the ICA, BA, and IMCA, and rMCA. 2DRF acquisitions were reconstructed without UNFOLD (line 1) or with UNFOLD with $E_f=0.5N_y$ (line 2) or $E_f=0.8N_y$ (line 3).

2DRF	Relative mean difference in peak flow $\frac{\overline{\hat{Q}_{2DRF}-\hat{Q}_{ref}}}{\overline{\hat{Q}_{2DRF}+\hat{Q}_{ref}}} (\%)$							
	RFL				RFS			
Artery	ICA	BA	IMCA	rMCA	ICA	BA	IMCA	rMCA
without UNFOLD	-3.1	-6.0	1.4	-3.2	-7.9	-11.9	-3.2	-8.0
	± 17.8	± 14.9	± 19.4	± 13.5	± 13.2	± 14.8	± 32.9	± 20.6
with UNFOLD	+0.7	-3.9	5.6	1.3	-4.2	-7.8	3.1	-3.8
$E_f=0.5N_y$	± 19.4	± 16.3	± 20.7	± 13.5	± 14.3	± 15.3	± 35.8	± 18.0
with UNFOLD	+2.0	0.8	7.6	2.3	-3.1	2.9	8.3	-1.3
$E_f=0.8N_y$	± 17.7	± 14.5	± 19.5	± 12.6	± 12.9	± 15.5	± 37.8	± 18.1

B Relative mean difference in peak velocity between 1DRF excitation and 2DRF excitations RFL or RFS for the ICA, BA, IMCA, and rMCA. 2DRF acquisitions were reconstructed without UNFOLD (line 1) or with UNFOLD with $E_f=0.5N_y$ (line 2) or $E_f=0.8N_y$ (line 3).

2DRF	Relative mean difference in peak velocity $\frac{\overline{\hat{v}_{2DRF}-\hat{v}_{ref}}}{\overline{\hat{v}_{2DRF}+\hat{v}_{ref}}} (\%)$							
	RFL				RFS			
Artery	ICA	BA	IMCA	rMCA	ICA	BA	IMCA	rMCA
without UNFOLD	-3.4	-7.5	13	-2.2	1.9	-16.0	18	-4.8
	± 12.5	± 24.2	± 19.7	± 15.9	± 7.8	$\pm 15.4^*$	$\pm 13.2^*$	± 20.9
with UNFOLD	0.4	-5.4	17	2.3	5.7	-11.9	24	-0.6
$E_f=0.5N_y$	± 14.3	± 23.8	$\pm 19.3^*$	± 17.5	± 9.4	± 15.1	$\pm 16.7^*$	± 19.4
with UNFOLD	1.8	-0.7	19	3.3	6.8	-7.0	30	1.9
$E_f=0.8N_y$	± 13.3	± 21.6	$\pm 19.3^*$	± 18.8	± 8.1	± 15.9	$\pm 18.3^*$	± 21.8

C Relative mean difference in peak flow between reconstructions without and with UNFOLD with $E_f=0.5N_y$ (line 1) or $E_f=0.8N_y$ (line 2) for 2DRF excitations RFL and RFS and the ICA, BA, IMCA, and rMCA.

2DRF	Relative mean difference in peak flow $\frac{\overline{\hat{Q}_{UNFOLD}-\hat{Q}}}{\overline{\hat{Q}_{UNFOLD}+\hat{Q}}} (\%)$							
	RFL				RFS			
Artery	ICA	BA	IMCA	rMCA	ICA	BA	IMCA	rMCA
with UNFOLD	3.8	2.1	4.2	4.5	3.7	4.1 \pm	6.6	4.3
$E_f=0.5N_y$	$\pm 2.7^*$	± 2.7	$\pm 2.6^*$	$\pm 2.7^*$	$\pm 2.4^*$	2.0*	± 5.3	$\pm 4.1^*$
with UNFOLD	5.2	6.8	6.2	5.5	4.9	9.1 \pm	11.9 \pm	6.7 \pm
$E_f=0.8N_y$	$\pm 2.4^*$	$\pm 4.4^*$	$\pm 2.2^*$	± 4.2	$\pm 1.4^*$	4.5*	7.5*	4.2*

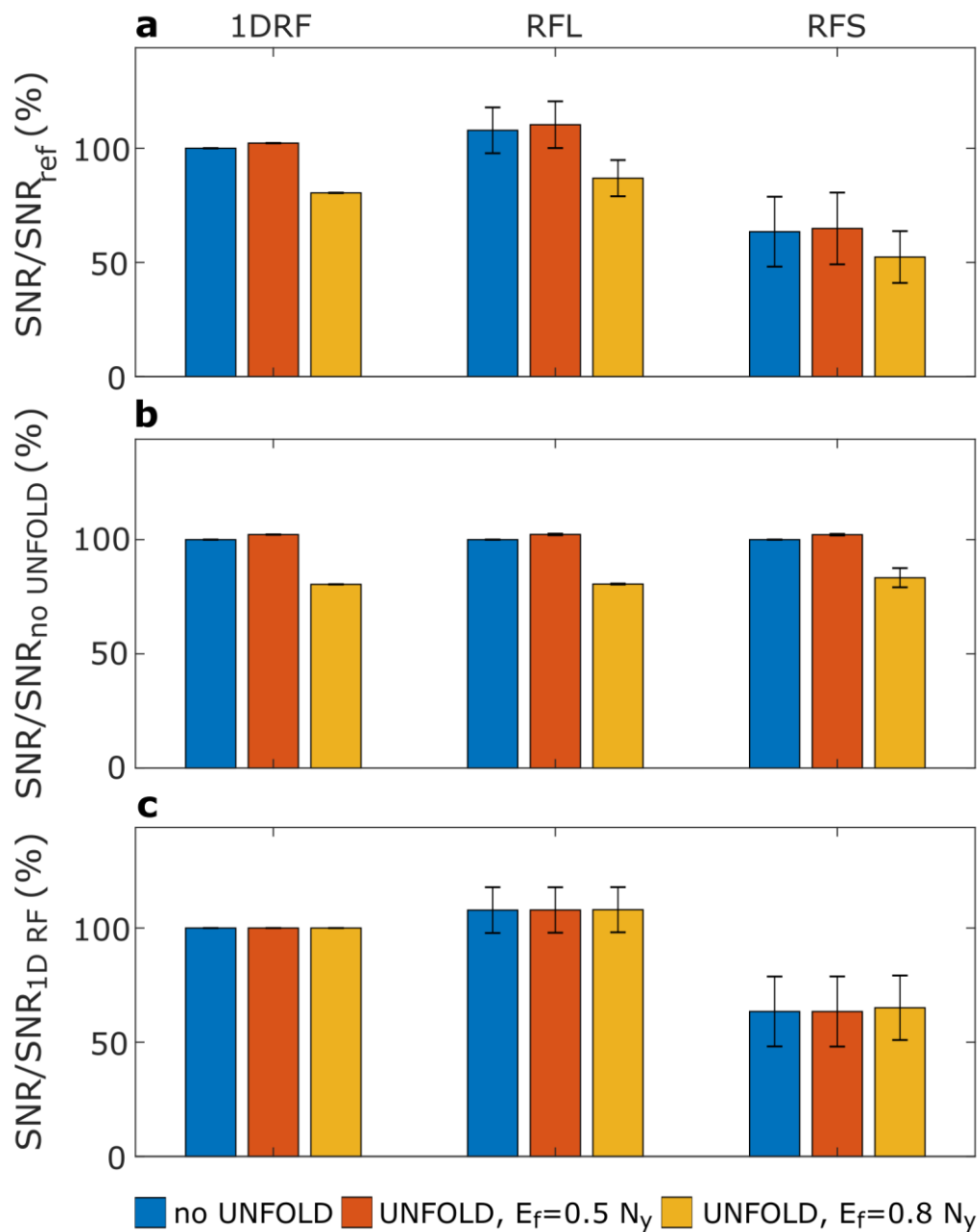
D Relative mean difference in blood flow volume per cardiac cycle between reconstructions without and with UNFOLD with $E_f=0.5N_y$ (line 1) or $E_f=0.8N_y$ (line 2) for 2DRF excitations RFL and RFS and the ICA, BA, IMCA, and rMCA.

2DRF	Relative mean difference in blood flow volume $\frac{\overline{V}_{\text{UNFOLD}-V}}{\overline{V}_{\text{UNFOLD}+V}}$ (%)							
	RFL				RFS			
Artery	ICA	BA	IMCA	rMCA	ICA	BA	IMCA	rMCA
with UNFOLD	-0.2	-0.2	0.1	-0.0	-0.2	-0.2	0.2	-0.2
$E_f=0.5N_y$	± 0.3	± 0.5	$\pm 0.1^*$	± 0.4	$\pm 0.2^*$	± 0.4	± 0.3	± 0.5
with UNFOLD	+0.2	0.0	0.3	0.3	+0.6	0.7 \pm	0.7	0.7
$E_f=0.8N_y$	± 0.5	± 1.0	$\pm 0.2^*$	± 0.5	$\pm 0.4^*$	0.6*	± 0.5	± 1.1

Abbreviations: BA, basilar artery; ICA, internal carotid artery; IMCA, left middle cerebral artery; rMCA, right middle cerebral artery

* $P \leq 0.05$

Supporting Information Figure S5:



Supporting Information Figure S5: Bar plots visualizing the SNR in static tissue for 1DRF (first column) and 2DRF RFL (second column) and RFS (third column). The corresponding data sets (III, I, and II) were reconstructed without (blue) and with UNFOLD using $E_f=0.5 N_y$ (red) and $E_f=0.8 N_y$ (yellow). **A**, The SNR relative to reference data set (III) without UNFOLD reconstruction and, **B**, the SNR relative to reconstruction without UNFOLD, and, **C**, the SNR relative to 1DRF in percentage. Error bars indicate the corresponding SD over all volunteers.